Oscillations of Sessile Drops of Surfactant Solutions on Solid Substrates with Differing Hydrophobicity

Maria von Bahr,† Fredrik Tiberg,‡ and Boris Zhmud*,†

Institute for Surface Chemistry YKI, Box 5607, SE-114 86 Stockholm, Sweden, and Camurus AB, Ideon Science Park, Sölvegatan 41, SE-223 70 Lund, Sweden

Received February 18, 2003

The paper reports results of experimental studies on the dynamic behavior of surfactant solution drops on substrates with differing hydrophobicity. Contact angle oscillations observed immediately after the drop deposition are studied, and a mechanistic interpretation of this phenomenon is put forward. The major emphasis is put on the physicochemical aspects of surfactant action, including the dynamic wetting enhancement and the effect of surface tension relaxation on the frequency of drop oscillation, which are characteristic of surfactant solutions. Appropriate scaling relations describing the drop dynamics are derived.

Introduction

The impact and spreading of solution drops on a solid target is a vital step in many technical applications, such as ink-jet printing, painting, and spraying of pesticides. Many processes are run at high speeds, and therefore it is of significant importance to understand and be able to control the dynamics of the drop spreading. To achieve the desired wetting characteristics, surfactants are often used in product formulation.

During the drop impact, provided that the drop hits the surface with a fairly high kinetic energy, the spreading is dominated by inertia. The liquid velocity in the radial direction at the impact time can be significantly higher than the impact velocity, but it soon reduces due to viscous dissipation and the transfer of energy to the expanding liquid/vapor interface.[1,2] If V is the drop volume, the drop expansion area can be estimated from the energy balance and, in the case of sufficiently viscous liquids and high-impact energies, scales as $V^{2/3}\mathrm{Re}^{1/2}$ where $\mathrm{Re} = V^{1/3}\rho v/\eta$ is the Reynolds number. Here, ρ is the density, η is the dynamic viscosity of the liquid, and v is the characteristic flow velocity. Capillary effects are negligible as long as $\mathrm{We} \gg \mathrm{Re}^{1/2}$, or equivalently, $\mathrm{WeCa} \gg 1$, where $\mathrm{We} = V^{1/3}\rho v^2/\gamma_{lv}$ is the Weber number (γ_{lv} being the surface tension of the liquid/vapor interface) and $\mathrm{Ca} = \mathrm{We}/\mathrm{Re}$ is the capillary number.[3]

After hitting the surface, the drop can splash on a hydrophilic surface or rebound after recoiling on a hydrophobic surface.[4] At smaller impact energies, oscillations of the sessile drops on hydrophobic substrates can be observed. When the impact energy is still fairly high, oscillations will move the three-phase contact line back and forth over the surface. At lower energies, only the top of the drop will oscillate and the three-phase contact line remains pinned to the surface due to the contact angle hysteresis.

Several studies have been performed to evaluate the effect of surfactants on the impact process.[3,5−8] Pasandideh-Fard et al. have shown that surfactants can increase the maximum spreading diameter, which is reached before the recoiling of the drop commences.[3] They also found that the recoil height decreased when a surfactant was added to the aqueous phase. In agreement with Pasandideh-Fard et al., Mourougou-Candoni et al. have shown that the droplet retraction is drastically influenced by adsorption kinetics of the surfactant.[6,7] Furthermore, Bergeron et al. have discovered that the presence of a small amount of a polymer in the solution inhibits the rebounding of drops on a hydrophobic solid.[9] Even though the shear viscosity and surface tension of dilute polymer solutions are very close to those of pure water, the polymer solution drops have a significantly lower retraction rate than the drops of pure water. Such behavior can be rationalized taking into consideration the non-Newtonian properties of polymer solutions and, in particular, the effect of polymer on the elongational viscosity.

At a later time after the impact, the spreading is dominated by surface tension forces (or gravity for larger drops) and viscosity. In the case of surfactant solutions spreading on hydrophobic substrates, it is often the adsorption of surfactant to the liquid/vapor and solid/liquid interfaces that controls the spreading dynamics. Under certain conditions, the surfactant can be transferred to the solid/liquid interface from the liquid/vapor interface via the three-phase contact line, although the direct exchange of surfactant between the solution phase and the solid/liquid interface always contributes to equilibrating the adsorbed layer. On the contrary, for substrates with low hydrophobicity, the three-phase contact line carryover does not play any significant role, though surfactant can still be adsorbed to the solid/liquid interface in a micellar form directly from solution.[10−13]

* To whom correspondence should be addressed.
† Institute for Surface Chemistry YKI.
‡ Camurus AB.

(1) Engel, O. G. *J. Res. Natl. Bur. Stand.* **1955**, *54*, 281.
(2) Levin, Z.; Hobbs, P. V. *Philos. Trans. R. Soc. London* **1971**, *A269*, 555.
(3) Pasandideh-Fard, M.; Qiao, Y. M.; Chandra, S.; Mostaghimi, J. *Phys. Fluids* **1996**, *8*, 650.
(4) Crooks, R.; Boger, D. V. *J. Rheol.* **2000**, *44*, 973.
(5) Zhang, X.; Basaran, O. A. *J. Colloid Interface Sci.* **1997**, *187*, 166.
(6) Mourougou-Candoni, N.; Prunet-Foch, B.; Legay, F.; Vignes-Adler, M.; Wong, K. *J. Colloid Interface Sci.* **1997**, *192*, 129.
(7) Mourougou-Candoni, N.; Prunet-Foch, B.; Legay, F.; Vignes-Adler, M.; Wong, K. *Langmuir* **1999**, *15*, 6563.
(8) Crooks, R.; Cooper-White, J.; Boger, D. V. *Chem. Eng. Sci.* **2001**, *56*, 5575.
(9) Bergeron, V.; Bonn, D.; Martin, J. Y.; Vovelle, L. *Nature* **2000**, *405*, 772.
(10) von Bahr, M.; Tiberg, F.; Zhmud, B. *Langmuir* **1999**, *15*, 7069.

10.1021/la030062d CCC: $25.00
Published on Web 10/28/2003

In the present work, the spreading dynamics of two different nonionic surfactants are compared, using one common surfactant of the polyoxyethylene glycol alkyl ether type ($C_{10}E_6$) and one silicon surfactant (M(DE_6OH)M) representing an adduct of polymethylsiloxane and polyoxyethylene glycol. A series of thiolate-modified gold surfaces with different hydrophobicity were used as substrates. Different stages of the drop spreading process were investigated. A special focus was made on studying the oscillatory behavior of drops following the impact.

Experimental Section

Methods. *Dynamic Contact Angle Measurements.* The contact angle measurements were performed with a DAT 1100 HS instrument (Fibro Systems AB, Sweden). The instrument is equipped with a video camera Mikrotron MC 1020, with an asynchronous shutter open for 0.64 ms and a pixel size of 10 × 10 μm, capable of taking 1000 images per second. The base diameter and height of the spreading drop are acquired from its profile. The drop contour is used in an iterative process to get the rotational 3-D volume of the drop and to calculate the average contact angle. The measurements were started when the drop was released from the tip of the Teflon tubing (inner and outer diameters of 0.2 and 0.7 mm, respectively) by a short stroke from an electromagnet. Care was taken that all interfaces in the syringe and Teflon tubing had been saturated with surfactant before the measurements started. The drop volume varied between 1.2 and 2.8 μL. All the spreading experiments were carried out in a climate-room at a temperature of 23 ± 1 °C and at a relative humidity of 50 ± 3%.

Dynamic Surface Tension Measurements. The surface tension dynamics (Figure 1) was measured by using a MPT2 maximum bubble pressure tensiometer (Lauda, Germany) or a pendent drop technique (First Ten Angstrom 200, USA). A detailed description of these two techniques can be found elsewhere.[14,15] With the maximum bubble pressure tensiometer, one can measure the dynamic surface tension in a time interval from 1 ms up to a few seconds, and the pendent drop technique is suitable in a time interval from a few seconds up to a few minutes. The interval from roughly 0.5 to 2 s proved to be notoriously difficult for performing accurate measurements with either instrument. The data (surface tension, γ_{lv}, vs time, t) within this interval were calculated directly from the volume of the pendant drop,

$$\gamma_{lv} = \beta(V)V^{2/3} \tag{1}$$

using extrapolated values of the conversion factor, $\beta(V)$. The latter had been calculated according to the empirical formula

$$\beta(V) = a_1 + \frac{a_2}{(V^{2/3} - a_3)^{a_4}} \tag{2}$$

having four fitting parameters, a_1, a_2, a_3, and a_4, chosen so as to reproduce the actual $\beta(V)$ dependence over an extended time interval where quite accurate pendant drop measurements were possible.

The critical micelle concentration (cmc) and the equilibrium surface tension for M(DE_6OH)M and two other analogous surfactants, M(DE_8OH)M and M(DE_{10}OH)M, were measured by a Sigma 70 Tensiometer (KSV Instruments Ltd., Finland) equipped with a platinum du Noüy ring and a titration unit (Metrohm, Switzerland). The equilibrium surface tension for concentrations well above cmc was 20 and 32 mN m^{-1} for M(DE_6-OH)M and $C_{10}E_6$, respectively.[10] All the measurements were performed at a temperature of 23 ± 1 °C.

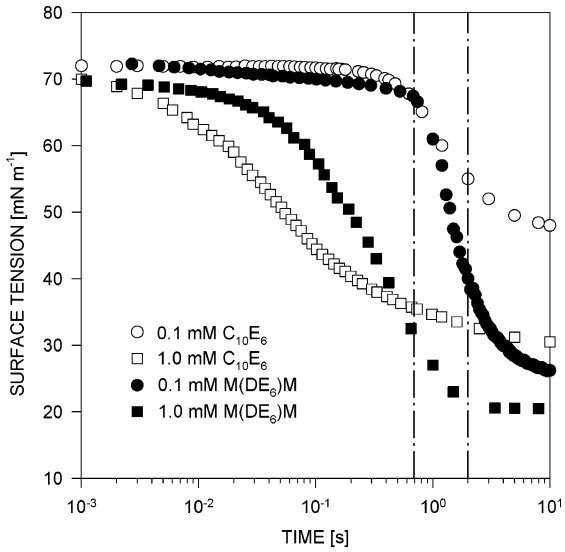

Figure 1. Surface tension relaxation dynamics for M(DE_6-OH)M and $C_{10}E_6$ surfactant solutions. The data points in the region flanked by the vertical lines were obtained using the extrapolation procedure described in the Experimental Section.

Materials. *Substrates.* The substrates used in this study were silicon wafers coated with a 10 Å titanium layer followed by a 100 Å gold layer. Then, a well-ordered mixed molecular monolayer of thiohexadecanol ($HS(CH_2)_{16}OH$) and thiohexadecane ($HS(CH_2)_{15}CH_3$) was adsorbed from an ethanol solution on the top of the gold layer in order to achieve the desired hydrophobicity. Details of the production process and the properties of the obtained surfaces have been described earlier.[10] The contact angle with water was regularly measured to ensure that the surface energy of the surfaces remained constant and that they were not contaminated.

Surfactants. The surfactants used in this study were monodisperse hexa(oxyethylene glycol) *n*-decyl ether, $C_{10}E_6$, with the formula n-$C_{10}H_{21}(OCH_2CH_2)_6OH$, and a trisiloxane surfactant, M(DE_6OH)M, with the formula $((CH_3)_3SiO)_2Si(CH_3)(CH_2)_3(OCH_2CH_2)_6OH$. For reference purposes, the adsorption parameters of two homologous products, M(DE_8OH)M and M(DE_{10}OH)M, were also determined. $C_{10}E_6$ was purchased from Nikko Chemicals Corp., and M(DE_nOH)M surfactants were kindly provided by Dow Corning Corp. All surfactants were used without further purification. The solutions were prepared by mixing the surfactant with double-distilled deionized water (Milli-Q system, Millipore). The values of the cmc were around 0.1 and 1 mM for M(DE_nOH)M and $C_{10}E_6$, respectively.[16]

Results and Discussion

Surfactant Adsorption. The adsorption of $C_{10}E_6$ and M(DE_nOH)M (n = 6, 8, 10) surfactants from aqueous solutions to the air/water interface has been studied using tensiometry. The adsorption parameters have been evaluated by fitting the theoretical surface tension versus concentration dependencies to the experimental data (see Figure 2). The fits were obtained using the generalized Frumkin adsorption isotherm,

$$\frac{\Gamma(c)}{\Gamma_m} = \frac{Kc}{Kc + \exp[p(\Gamma(c)/\Gamma_m)^q]} \tag{3}$$

(11) Zhmud, B.; Tiberg, F.; Hallstensson, K. *J. Colloid. Interface Sci.* **2000**, *228*, 263.
(12) Tiberg, F.; Zhmud, B.; Hallstensson, K.; von Bahr, M. *Phys. Chem. Chem. Phys.* **2000**, *2*, 5189.
(13) Eriksson, J.; Tiberg, F.; Zhmud, B. *Langmuir* **2001**, *17*, 7274.
(14) Miller, R.; Fainerman, V. B.; Schano, K.-H.; Hofmann, A.; Heyer, W. *Tenside, Surfactants, Deterg.* **1997**, *34*, 357.
(15) Adamson, A. W. *Physical Chemistry of Surfaces*, 5th ed.; Wiley: New York, 1990.
(16) Zhmud, B. V.; Tiberg, F.; Kizing, J. *Langmuir* **2000**, *16*, 2557.

where $\Gamma(c)$ is the equilibrium surface excess of surfactant when its bulk concentration equals c, Γ_m is the adsorption monolayer capacity, K is the adsorption equilibrium constant, and p and q are certain empirical parameters needed to take account of adsorbate−adsorbate interactions. The factor p reflects the energy of lateral interactions and the exponent q reflects a nonlinear increase in the strength of lateral interactions, which is a likely consequence of structural reorganization of the interfacial layer in the course of adsorption. The Langmuir adsorption isotherm represents an especial case of eq 3, where $p = 0$ and $q = 1$. Since Frumkin's isotherm offers a greater flexibility in fitting, it was considered a preferred choice.

In the $M(DE_nOH)M$ series of surfactants, the adsorption properties proved to be almost the same for $n = 6$, 8, and 10. A large negative value of the parameter p may be attributed to a strong cooperative effect due to the ordering of polysiloxane chains in the adsorbed layer. However, there still exists a significant deviation between the fitted curve and experimental data in the low-concentration region. This can be explained by insufficient equilibration time. For diffusion-controlled adsorption, the equilibration time, τ, increases with decreasing surfactant concentration,

$$\tau_{eq} \propto \frac{1}{10^6 D}\left(\frac{\Gamma_m K}{1 + Kc}\right)^2 \qquad (4)$$

where D is the diffusion coefficient of surfactant in solution. The latter estimate is obtained from the condition that the surfactant adsorbed needs to path through a diffusion zone, the thickness of which is increasing with time as $(Dt)^{1/2}$, and therefore, the following scaling relation holds, $c(D\tau_{eq})^{1/2} \simeq \Gamma(c)$. For example, for $D = 10^{-9}$ m^2 s^{-1} and $c = 10^{-4}$ mol dm^{-3}, it takes around 1 s for an equilibrium to be achieved, while for $c = 10^{-6}$ mol dm^{-3}, it would already take around 1 h. It has also been reported that at very low concentrations, $M(DE_6OH)M$ surfactant can form water-rich isotropic phases.[17]

Sessile Drop Oscillations: An Heuristic Interpretation. When a liquid drop hits a smooth solid surface, it is deformed under the action of inertia and surface forces. The kinetic energy the drop had before the impact is partly transformed into the surface energy of expanding liquid/vapor interface and partly dissipated due to viscous forces. After a certain relaxation time, the drop will attain an equilibrium configuration characterized by a contact angle, θ_{eq}. However, at the instant the drop touches the surface, the contact angle is close to 180°, that is, greater than the equilibrium value. Hence, the spreading tension, $\varphi = \gamma_{lv}[\cos\theta_{eq} - \cos\theta]$, where γ_{lv} is the surface tension of the liquid/vapor interface, initially acts in the same direction as the hydrodynamic pressure created on impact, and hence they both favor drop spreading. However, for sufficiently heavy and low-viscous liquids, the spreading drop will likely run past its equilibrium configuration due to the inertia and turns into another out-of-equilibrium configuration with a contact angle lower than θ_{eq}. In this case, the spreading tension will act in the opposite direction forcing the drop margin to contract. Therefore, damping oscillations of the contact angle will be observed until all the excess kinetic energy is dissipated.

Contact angle oscillations are not necessarily accompanied by movement of the drop margin. In fact, the latter can be fixed and standing capillary waves can be induced at the surface as shown below. In general, an

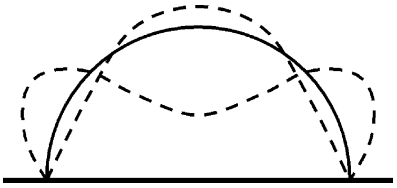

infinite number of wavelengths can exist; however, waves of shorter length will damp faster. For sufficiently spread drop configurations, this problem becomes similar to the problem of capillarity-driven liquid film leveling.

In fluid mechanics, a lot of effort has been put into studying the problems associated with fluid particle deformation and many elegant mathematical results have been obtained. The main difficulty in the theoretical analysis of problems of this type is that as the drop shape is deformed from the normal stress balance condition on the drop surface, the governing dynamic equations become nonlinear. Further, as drop oscillations are concerned, the nonlinear terms in the Navier−Stokes equation also need to be retained. Simultaneous solution of the nonlinear flow fields and the equation of the interface is a tremendously difficult task.[18] Significant progress here has been achieved using numerical simulations.[19]

In the present work, a phenomenological interpretation of the oscillatory behavior of sessile drops is given. Let ξ be the characteristic linear displacement from the equilibrium drop shape caused by drop deformation on impact. The impact energy is assumed to be so small that the drop is only slightly deformed. Then, ξ can, for example, be defined as the deviation from the equilibrium height of the drop, that is,

$$\xi = r_V(\theta_{eq})[1 - \cos\theta_{eq}] - r_V(\theta)[1 - \cos\theta] \qquad (5)$$

where r_V is the radius of the spherical cap of a sessile drop with the volume V and the contact angle θ,

$$r_V(\theta) = \left(\frac{3V}{\pi[2 - 3\cos\theta + \cos^3\theta]}\right)^{1/3} \qquad (6)$$

Neglecting the actual (in general, very complex) hydrodynamics of the drop, a simplified equation for the contact angle oscillations can be obtained, which, despite its phenomenological and grossly oversimplified character, will be seen to provide a qualitatively correct physical description of the phenomenon.

The term representing the liquid acceleration under the action of an external force, represented by a tensional part and a viscous part, will scale as $\rho V \ddot{\xi}$, where dots mean differentiation by time. The tensional part, which drives the spreading process, scales as $V^{1/3}\varphi = V^{1/3}\gamma_{lv}(\mathrm{d}\cos\theta/\mathrm{d}\xi)|_{\theta=\theta_{eq}}\xi$, provided that ξ is small. The viscous part, on the contrary, resists spreading. The amount of energy dissipated due to viscous drag scales as

$$\int \mathrm{d}t \int \mathrm{d}V\eta\left(\frac{\partial v_i}{\partial x_j} + \frac{\partial v_j}{\partial x_i}\right)^2 \propto \eta V^{2/3}\dot{\xi} \qquad (7)$$

(17) *Silicone Surfactants*; Hill, R. M., Ed.; Marcel Dekker: New York, 1999.

(18) Zapryanov, Z.; Tabakova, S. *Dynamics of Bubbles, Drops and Rigid Particles*; Kluver Academic Publishers: Dordrecht, 1999.

(19) Fukai, J.; Zhao, Z.; Poulikakos, D.; Megaridis, C. M.; Miyatake, O. *Phys. Fluids* **1993**, *5*, 2588.

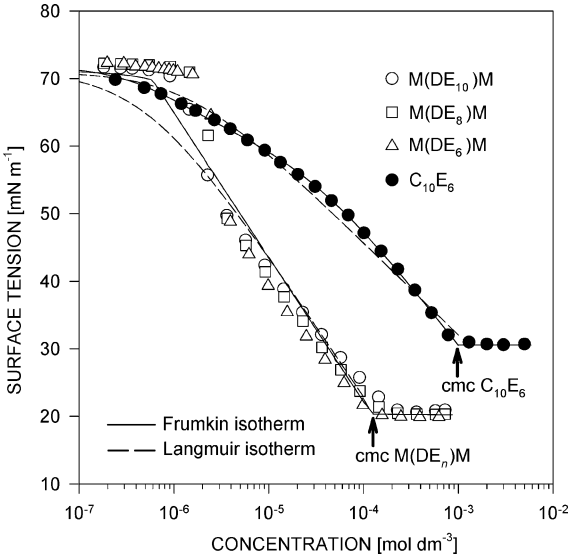

Figure 2. Determination of adsorption parameters for M(DE$_n$OH)M and $C_{10}E_6$ surfactants. M(DE$_n$OH)M surfactants: $\Gamma_m = 3.7 \times 10^{-6}$ mol m^{-2}, $K = 2.4 \times 10^5$ dm^3 mol^{-1}, $p = -9.0$, and $q = 1.7$ for the Frumkin isotherm; $\Gamma_m = 4.2 \times 10^{-6}$ mol m^{-2} and $K = 1.1 \times 10^6$ dm^3 mol^{-1} for the Langmuir isotherm. $C_{10}E_6$ surfactant: $\Gamma_m = 2.9 \times 10^{-6}$ mol m^{-2}, $K = 1.4 \times 10^6$ dm^3 mol^{-1}, $p = 3.7$, and $q = 1.7$ for the Frumkin isotherm; $\Gamma_m = 2.4 \times 10^{-6}$ mol and $K = 7 \times 10^5$ dm^3 mol^{-1} for the Langmuir isotherm.

where $\mathbf{v} = (v_1, v_2, v_3)$ is the velocity field inside the drop. Therefore, the drag force itself should scale as $\eta V^{1/3}\dot{\xi}$. V does not necessarily represent the entire volume of the drop. For a sufficiently spread drop configuration, the energy dissipation will mostly occur near the drop margin. However, because of the heuristic character of the presented analysis, not aimed at quantitative results, all the geometry-dependent factors can be simply replaced by unity, leading to the following equation for the contact angle oscillations:

$$\ddot{\theta} + \frac{2\eta}{\rho V^{2/3}}\dot{\theta} + \frac{\gamma_{lv}}{\rho V}(\theta - \theta_{eq}) = 0 \qquad (8)$$

In its derivation, relation 5 between the contact angle, θ, and the linear displacement, ξ, has been used, assuming that ξ is small. The solution to this equation can be presented in the form

$$\theta = \theta_{eq} + \epsilon \exp\left(-\frac{\eta t}{\rho V^{2/3}}\right) \cos\left[\left(\frac{\gamma_{lv}}{\rho V} - \frac{\eta^2}{\rho^2 V^{4/3}}\right)^{1/2} t\right] \qquad (9)$$

where ϵ is the initial amplitude of oscillations. This shows that the frequency of oscillations is proportional to the square root of the surface tension and decreases with time as oscillations damp down; a greater viscosity aids faster damping. There always exists a certain critical drop size, d, below which no oscillation is possible,

$$d \simeq \frac{\eta^2}{\rho\gamma_{lv}} \qquad (10)$$

For water, $\eta = 10^{-3}$ Pa s; $\gamma_{lv} = 7 \times 10^{-2}$ N m^{-1} and $\rho = 10^3$ kg m^{-3}, and hence, $d \cong 10$ nm. Also, there always exists a certain critical viscosity above which no oscillation is possible. The estimated frequency of oscillation of a 2 μL water drop has the order of magnitude of $(\gamma_{lv}/\rho V)^{1/2} \sim 200$ s^{-1}, which corresponds to the oscillation period of 5 ms. Adsorption of surfactant and concomitant surface tension relaxation entail an increase in the oscillation period to 8 ms. This is in reasonable agreement with the experiment. However, the characteristic damping time is grossly overestimated, $\rho V^{2/3}/\eta \sim 1$ s. In practice, the oscillation damping occurs much faster than predicted by the above equation (see Figures 3 and 4). This can be explained by the existence of additional (not allowed for in the present model) damping factors such as the contact line friction,[20,21] internal vortices, and the viscous dissipation in air.

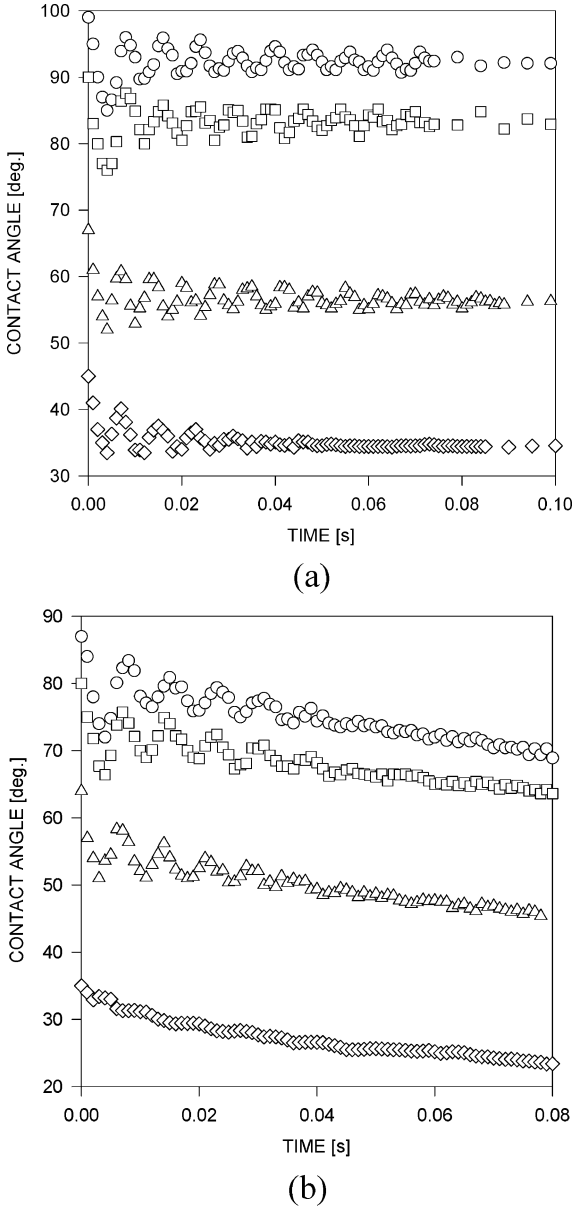

Figure 3. Contact angle oscillations after the drop deposition onto the surface: (a) 0.1 mM M(DE$_6$OH)M surfactant solution; (b) 1.0 mM M(DE$_6$OH)M surfactant solution. The drop volume is ca. 2.5 μL. The surface hydrophobicity decreases from the top to the bottom following the hydroxyl/alkyl ratio: (○) 0:100 OH/CH$_3$, (□) 25:75 OH/CH$_3$, (△) 50:50 OH/CH$_3$, and (◇) 75:25 OH/CH$_3$.

Equations 8 and 9 turn out to be of more general character than the assumptions used in their derivation. In particular, they cover the case of contact angle oscillations observed for sessile drops with a pinned three-

(20) de Ruijter, M. J.; Charlot, M.; Voué, M.; de Coninck, J. *Langmuir* **2000**, *16*, 2363.
(21) Kolev, V. L.; Kochijashky, I. I.; Danov, K. D.; Kralchevsky, P. A.; Broze, G.; Mehreteab, A. *J. Colloid Interface Sci.* **2003**, *257*, 357.

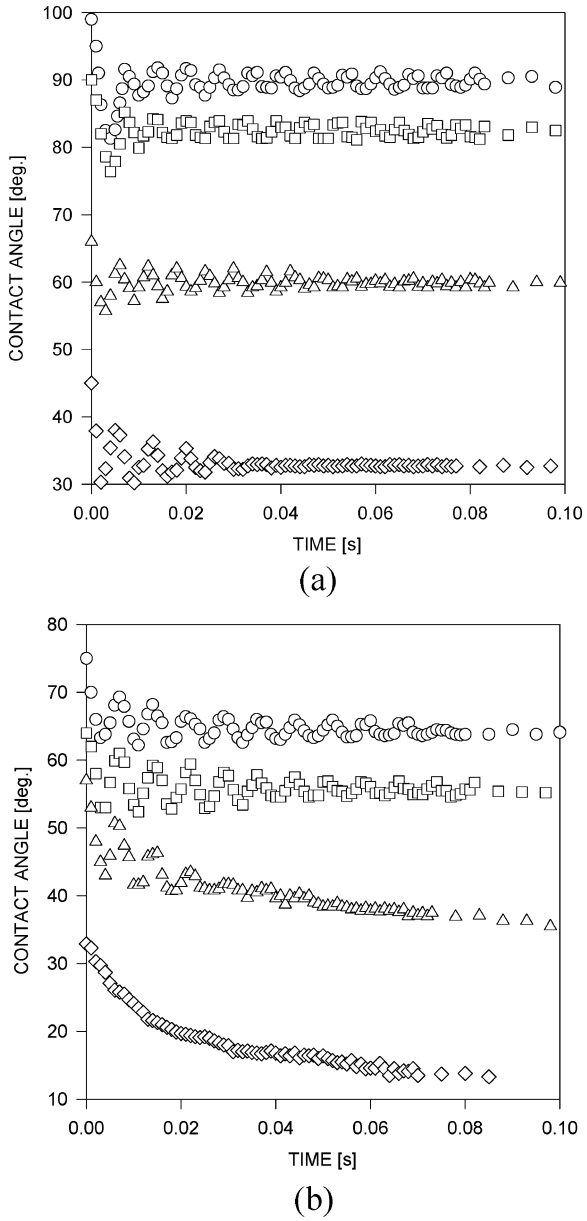

Figure 4. Contact angle oscillations after the drop deposition onto the surface: (a) 0.1 mM $C_{10}E_6$ surfactant solution; (b) 1.0 mM $C_{10}E_6$ surfactant solution. The drop volume is ca. 2.5 μL. The surface hydrophobicity decreases from the top to the bottom following the hydroxyl/alkyl ratio: (○) 0:100 OH/CH_3, (□) 25:75 OH/CH_3, (△) 50:50 OH/CH_3, and (◇) 75:25 OH/CH_3.

phase contact line. In the latter case, the role of the elastic force is played by local deviations of the Laplace pressure from its equilibrium value corresponding to the hemispherical geometry of the nondeformed drop cap. This gives a term proportional to $\gamma_{lv}V^{1/3}(\theta - \theta_{eq})$, whereas the viscous dissipation term remains the same as before, $\eta V^{2/3}\dot{\theta}$. Once the amplitude of the oscillations is assumed to be small, the role of the surface tension gradients associated with periodic expansion/contraction of the adsorbed film is negligible. However, a small anharmonicity in the oscillations should be expected.

An interesting case is the study of drops of a surfactant solution for which the surface tension relaxation is slower than the oscillation damping. In this case, one can use quasi-stationary (i.e., slowly changing with time) values of the parameters γ_{lv} and θ_{eq} for describing the oscillations and the early stages of the drop spreading and the equilibrium values for describing the late stages of the

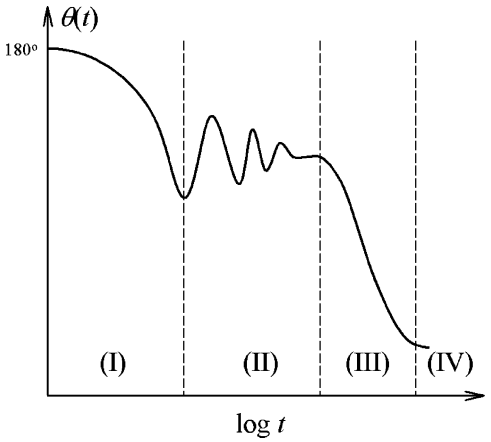

Figure 5. Different possible stages of the drop spreading process.

drop spreading and the final drop configuration. The quasi-equilibrium surface tensions and the contact angle can be found from the Gibbs and Young−Dupré equations, respectively:

$$\gamma_{sl}(t) = \gamma_{sl}^0 - RT\int_0^{c(\mathbf{r},t)|_{sl}} \Gamma_{sl}\, d\ln c \qquad (11)$$

$$\gamma_{lv}(t) = \gamma_{lv}^0 - RT\int_0^{c(\mathbf{r},t)|_{lv}} \Gamma_{lv}\, d\ln c$$

$$\theta_{eq}(t) = \arccos\frac{\gamma_{sv} - \gamma_{sl}(t)}{\gamma_{lv}(t)} \qquad (12)$$

where the subscripts sv and sl refer to the solid/vapor and solid/liquid interfaces, respectively, and $c(\mathbf{r},t)|_s$ is the concentration of surfactant near the corresponding interface.

If the relaxation rates for the drop oscillations and for the surface tension are of the same order of magnitude, eq 8 has time-dependent coefficients and can only be solved numerically.

The drop is always to some extent pre-equilibrated before having been deposited to the substrate, and hence, it is only the long-time phase of the surface tension relaxation process that superimposes on the drop spreading process in time. Thus, already at the beginning of the spreading process, the surface tension of the liquid/vapor interface is likely to be close to its equilibrium value for a given surfactant concentration. However, the adsorption to the solid/liquid interface can remain a rate-limiting stage at early stages of the contact angle dynamics.

Based on the results obtained, several different stages in the drop spreading process can be distinguished as shown in Figure 5.

Stage I. The drop touches the surface and begins to spread under the action of the gravity, surface tension, and inertia forces. The gravity can be neglected if the drop diameter $d \ll (\gamma_{lv}/\rho g)^{1/2}$. Depending on the substrate wettability, liquid viscosity, drop size, and surface tension relaxation rate, the contact angle may or may not fall below its quasi-equilibrium value determined by the momentary balance of surface tensions at the three-phase contact line. In this time window, $\gamma_{lv}(t) \simeq \gamma_{lv}(\infty)$ if the pendant drop has been pre-equilibrated and $\gamma_{sl}(t) \simeq \gamma_{sl}(0)$ if the surface tension relaxation time (see eq 4) is greater than the time passed since the moment of the impact. However, for polymeric surfactants and surfactants with extremely low cmc, the drop formation and delivery time may happen to be much shorter than the surface tension

relaxation time, in which case $\gamma_{lv}(t) \simeq \gamma_{lv}(0)$. If, furthermore, the characteristic spreading time, $\tau_{sp} = \eta V^{1/3}/(\gamma_{lv}\theta^{10/3})$, is much shorter than the surface tension relaxation time, $\tau_{eq} \gg \tau_{sp}$(see eq 4), a quasi-equilibrium contact angle can be attained.

Stage II. The contact angle oscillates around its quasi-equilibrium value until the kinetic energy is dissipated by viscous friction. The existence and duration of oscillations depend on the size of the drop, viscosity, and surface tension of the liquid and the wettability of the substrate. Inertia plays an important role throughout stages I and II. A surface excess of surfactant at the sl and lv interfaces gradually mounts up due to adsorption, causing a downward drift of the quasi-equilibrium contact angle.

Stage III. The excess kinetic energy has been dissipated, and the surface tension of the sl and lv interfaces dropped to a level enabling further drop spreading. Depending on solution viscosity and surfactant diffusivity and adsorption affinity for lv and sl interfaces, a diffusion-controlled spreading regime or the creeping flow regime may take over. In the creeping flow regime, the spreading rate is determined by a momentary balance between the spreading tension and viscous drag. The drop deformation is assumed to be slow enough to maintain γ_{lv} and γ_{sl} at their equilibrium values. From a hydrodynamic viewpoint, the creeping flow regime is characterized by simultaneously small values of the Reynolds (Re), Bond (Bo), and Schmidt (Sc) numbers.

Stage IV. Because the amount of surfactant in a drop of a finite size is limited, at some point it is depleted by adsorption. At this point, the spreading stops. The corresponding equilibrium contact angle can be calculated using the Young−Dupré equation in combination with the mass balance constraint,

$$S_{lv}\Gamma_{lv}(c) + S_{sl}\Gamma_{sl}(c) = (c_0 - c)V \qquad (13)$$

$$S_{lv} = 2\pi r_V^2(1 - \cos\theta_\infty)$$

$$S_{sl} = \pi r_V^2 \sin^2\theta_\infty$$

For example, a 2.5 μL drop of 0.1 mM surfactant solution can be expected to spread on a hydrophobic substrate over an area of about $S_{sl} \simeq 0.5$ cm^2, after which the spreading stops. The corresponding contact angle is $\theta_\infty \simeq 4\pi^{1/2}S_{sl}^{-3/2}V \simeq 3°$.

So far, it has tacitly been assumed that adsorbed surfactant is instantly redistributed over the lv interface so that the surface tension γ_{lv} is only a function of time but not coordinates. However, in reality, it is the drop margin that is primarily depleted of surfactant, and therefore, the surface tension near the margin will in general be higher than that in the center of the drop. This gives rise to a Marangoni flow in the radial direction. Under such conditions, the stress balance at the lv interface reads

$$\left\{p_l - p_v - \gamma_{lv}\left(\frac{1}{r_1} + \frac{1}{r_2}\right)\right\}\mathbf{n} = (\eta_l\mathbf{E}_l - \eta_v\mathbf{E}_v)\cdot\mathbf{n} + \nabla_S\gamma_{lv} \qquad (14)$$

where η_i (i = l, v) are the viscosities of the fluids l and v, respectively, $\mathbf{n}$ is the unit normal, and $\mathbf{E}_i$ (i = l, v) are the strain tensors expressed through velocity fields in the fluids l and v,

$$E_{\alpha\beta} = [\nabla\mathbf{v} + (\nabla\mathbf{v})^T]_{\alpha\beta} = \frac{\partial v_\alpha}{\partial x_\beta} + \frac{\partial v_\beta}{\partial x_\alpha} \quad (\alpha,\beta = 1,2,3) \qquad (15)$$

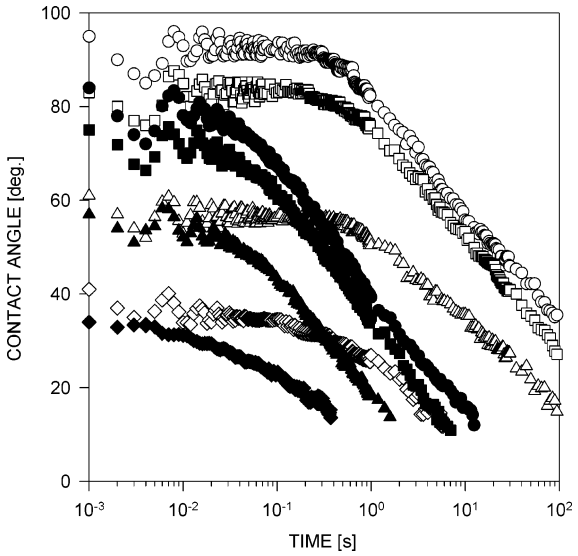

Figure 6. Contact angle dynamics for M(DE$_6$OH)M surfactant solution drops spreading on substrates with varying hydrophobicity: (○) 0:100 OH/CH$_3$, (□) 25:75 OH/CH$_3$, (△) 50:50 OH/CH$_3$, and (◇) 75:25 OH/CH$_3$. The surfactant concentration is 0.1 mM (empty figures) and 1.0 mM (filled figures). The drop volume is ca. 2.5 μL.

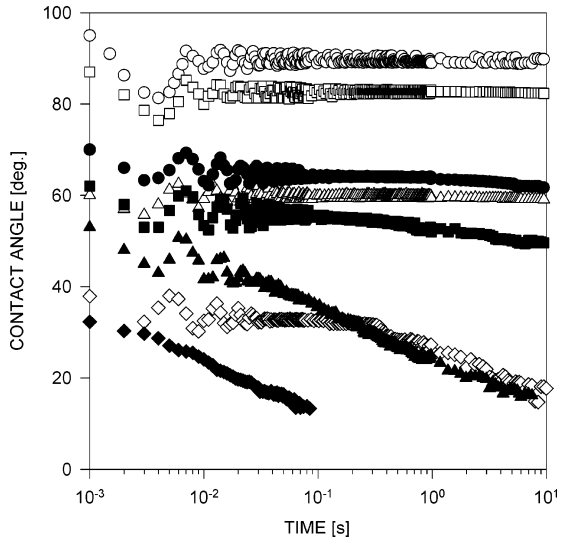

Figure 7. Contact angle dynamics for $C_{10}E_6$ surfactant solution drops spreading on substrates with varying hydrophobicity: (○) 0:100 OH/CH$_3$, (□) 25:75 OH:CH$_3$, (△) 50:50 OH/CH$_3$, and (◇) 75:25 OH/CH$_3$. The surfactant concentration is 0.1 mM (empty figures) and 1.0 mM (filled figures). The drop volume is ca. 2.5 μL.

Equation 14 is obviously a generalization of the Laplace equation. In the presence of the surface tension gradient, $\nabla_S\gamma_{lv}$, the drop shape will deviate from a spherical cap as the spreading proceeds. Such deviations have been experimentally observed by other researchers.[22] The tangential force associated with adsorption-related surface tension gradients is

$$\frac{\partial\gamma_{lv}}{\partial\Gamma_{lv}}\nabla_S\Gamma_{lv} \qquad (16)$$

To calculate the gradient in the surface excess, Γ_{lv}, of surfactant, the corresponding transport equation,

$$\frac{\partial c}{\partial t} + \nabla\cdot(c\mathbf{v}) = D\nabla^2 c \qquad (17)$$

must be solved together with the Navier−Stokes equation of fluid dynamics with appropriate boundary conditions reflecting the surfactant adsorption dynamics. This complex problem, involving moving boundaries, is far beyond the scope of the present communication.

As can be seen in Figures 6 and 7, the extent of spreading for the $M(DE_6OH)M$ solutions is larger than for the $C_{10}E_6$ solutions, which is due to the fact that at equal concentrations the former has a lower equilibrium surface tension than the latter. As can be expected, this effect is more pronounced on hydrophobic substrates. On the most hydrophobic substrates, the spreading rate of 1 mM $M(DE_6OH)M$ solution drops is faster than that of 1 mM $C_{10}E_6$ solution drops. On the substrate with a 50:50 OH/CH_3 composition, the spreading rates are similar for both surfactants. Finally, on the most hydrophilic substrates, the spreading rate of $C_{10}E_6$ solution drops becomes greater than that of $M(DE_6OH)M$ solution drops, because the spreading tension is higher in the first case. This clearly shows that for the hydrophobic substrates, the spreading dynamics is affected by surfactant adsorption to both the solid/liquid and liquid/vapor interfaces, while for the hydrophilic substrates, it is only the adsorption to the liquid/vapor interface that plays a role.

Last, on the 75:25 OH/CH_3 substrate, a tendency toward a fitful spreading has been observed for both 0.1 mM $M(DE_6OH)M$ and 0.1 mM $C_{10}E_6$ solutions, which probably indicates some surface heterogeneity.

Acknowledgment. This research was carried out in the framework of the Nordic R&D project “Innovative Development of the Inkjet Technology” financed by the Nordic Industrial Fund. The work of M.v.B. was supported by the Swedish Pulp and Paper Research Foundation.

LA030062D

(22) Rafai, S.; Sarker, D.; Bergeron, V.; Meunier, J.; Bonn, D. *Langmuir* **2002**, *18*, 10486.